Desalination and Water Treatment
www.deswater.com
doi: 10.1080/19443994.2013.803319

52 (2014) 4527–4537
June

Taylor & Francis
Taylor & Francis Group

Enhanced adsorption of methylene blue on modified silica gel: equilibrium, kinetic, and thermodynamic studies

Atul Kumar Kushwaha[a,b,*], Neha Gupta[b], M.C. Chattopadhyaya[b]

[a]*Department of Chemistry, Lovely Professional University, Phagwara, Punjab, India*
Tel. +91 0532 2462393; email: atulkk2008@gmail.com
[b]*Department of Chemistry, University of Allahabad, Allahabad 211002, UP, India*

Received 31 May 2012; Accepted 20 April 2013

ABSTRACT

The present work was undertaken to chemically modify silica gel (SG) with citric acid (CA) to enhance its adsorption power for methylene blue (MB) dye from aqueous solution. Citric acid-modified silica gel (CAMSG) was synthesized thermochemically and was characterized by Fourier transform infrared (FT-IR) spectroscopy, scanning electron microscopy (SEM), and elemental analysis. Influences of various parameters such as adsorbent dose, pH, initial dye concentration, contact time, and temperature on adsorption were studied. Equilibrium data were analyzed using Langmuir, Freundlich, and Temkin isotherm models. Kinetic studies show that the adsorption follows pseudo-second-order kinetics and intraparticle diffusion model. Negative values of Gibb's free energy change (ΔG°) show that the adsorption was feasible and spontaneous in nature and the negative values of enthalpy change (ΔH°) confirm exothermic adsorption.

Keywords: Adsorption; Isotherm; Kinetics; Methylene blue; Silica gel

1. Introduction

Effluents from several industries (e.g. textile, leather, paper, pulp, plastics, food, etc.) contain huge amount of dyes and pigments used for coloring their final products. Dyes present in waste water may cause serious environmental pollution problems (e.g. reducing light penetration in water and photosynthesis). In addition, some dyes are either toxic or mutagenic and carcinogenic.

Methylene blue (MB) (C.I. Basic blue 9) is a cationic dye (Fig. 1). The toxic effects of MB dye are not that acute but it can cause several adverse effects on human beings e.g. it can damage cardiovascular, central nervous system, dermatologic, gastrointestinal, genito-urinary, hematologic system, etc. Hence, it is necessary to remove it from effluent discharge.

Various processes have been proposed for the removal of dyes from aqueous solution. The important ones are biodegradation, adsorption/precipitation [1], coagulation–flocculation [2], chemical oxidation [3], biological oxidation [4], electrochemical oxidation [5], membrane separation [6], and ultrafiltration [7]. Among these, the adsorption process is found to be quite suitable, cheap, and effective for the removal of dyes from aqueous solution. A considerable amount of work has also been published in the literatures regarding the adsorption of MB dye on various adsorbent surfaces such as alumina [8], clay [9–11], zeolite

*Corresponding author.

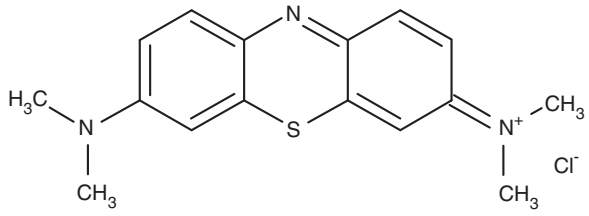

Fig. 1. Molecular structure of MB dye.

[12], peat [13], activated carbon [14], silica [15], organic polymers [16], algae [17], plants wastes [18–20], wood sawdust [21] agricultural waste materials [22,23], nanocomposites [24], organic–inorganic hydrogel composites [25], and nanotubes [26].

Availability of silica is in plenty and its high potential towards the adsorption of organic and inorganic compounds has attracted the attention of many researchers to use it in the removal of pollutants. The presence of –OH groups on the surface of the silica gel (SG) creates a site for the adsorption of cationic dye. In order to get high adsorption, SG was esterified with citric acid (CA) causing an increase in anionic adsorption site ($–COO^-$) on SG surface. In the present work, the adsorption properties of the activated silica gel (ASG) (Fig. 2(a)) and citric acid-modified silica gel (CAMSG) (Fig. 2(b)) were investigated with the cationic dye MB as target pollutant from aqueous solution as a function of pH, adsorbent dose, initial dye concentration, contact time, and temperature.

2. Methodology

2.1. Synthesis of adsorbent

Silica gel G (SG) was obtained from Sigma-Aldrich Chemicals Pvt. Ltd., India. Activation of SG was done by adding 100 mL of 6 M HCl in 20 g of SG and the mixture was allowed to reflux with continuous stirring for 4 h. The resultant material was filtered and washed with deionized water until the pH becomes seven and dried at 150°C for 5 h. The resulting material (ASG) was kept in a dessicator for use as an adsorbent.

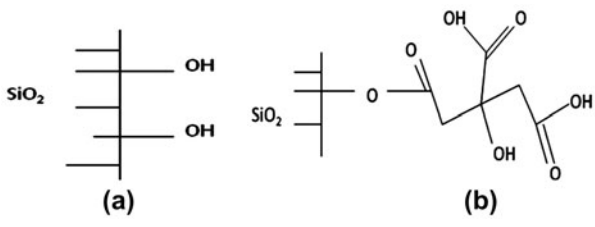

Fig. 2. Activated SG (a) and CAMSG (b).

The SG was modified with CA (Merck, India) by a similar procedure reported by Vaughan et al. [27]. Twenty gram of ASG was added into 0.6 M CA solution (1:12 w/v) in 500 mL flask. The resulting mixture was stirred for 30 min to make slurry, which was poured on stainless steel tray and was kept at 50°C for 24 h in forced air oven followed by an increase in temperature up to 120°C, where thermochemical reaction between SG and CA takes place. After cooling, the resulting material was washed with deionized water until the liquid did not turn turbid when 0.1 mol lead (II) nitrate was dropped in. After filtration, the solid was dried in an oven at 70°C. The resulting material (CAMSG) was kept in a dessicator for use as an adsorbent.

2.2. Preparation of cationic dye solutions

MB dye was obtained from Central Drug House Pvt. Ltd., India and was used without further purification. A stock solution of 1,000 mg L^{-1} of MB was prepared by dissolving 1 g of MB into 1 L of deionized water. It was subsequently diluted to different concentrations (20, 40, 60, 80, 100, and 150 mg L^{-1}) and the pH of dye solutions were maintained by adding 0.1 M HCl or 0.1 M NaOH. The experiments were carried out by taking 50 mL of MB solution and a required amount of adsorbent into 150 mL conical flasks and stirred using a magnetic stirrer (Remi) at a speed of 200 rpm. The adsorption was monitored by determining the concentration of MB in solution by double-beam UV–Visible spectrophotometer (Systronics-2203) at λ_{max} 665 nm.

The percentage of dye removal and quantity of MB adsorbed on adsorbent at the time of equilibrium (q_e) was calculated by Eqs. (1) and (2), respectively.

$$\% \text{ MB removal} = 100\ (C_0 - C_e)/C_0 \quad (1)$$

$$q_e = (C_0 - C_e)V/W \quad (2)$$

where C_0 and C_e are the initial and the equilibrium concentrations (mg/L) of MB in solution, q_e is quantity of MB adsorbed on the adsorbent at the time of equilibrium (mg/g), V is volume (L) of solution, and W is mass of adsorbent (g) taken for experiment.

Batch experiments were carried out to determine the effects of pH, adsorbent dose, initial dye concentration, contact time, and temperature by varying the parameter under study and keeping other parameters constant.

3. Results and discussion

3.1. Characterization of adsorbents

The Fourier transform infrared (FT-IR) spectra of ASG and CAMSG were recorded by FTLA2000 spectrophotometer using KBr disc method and are shown in Fig. 3. FT-IR spectra of ASG showed a band at 1,027 cm^{-1} which was due to asymmetric stretching of Si–O–Si and the corresponding symmetric stretching was observed at 805 cm^{-1}. The peak at 3,473 and 1,594 cm^{-1} was due to the stretching and bending of O–H groups and water molecules present in silica. The FT-IR spectra of CAMSG showed a band around 1,740 cm^{-1} formed due to stretching of C = O group of ester which confirms esterification of ASG with CA. The significant change was observed in surface morphology of ASG after its modification with CA as shown in scanning electron microscopy (SEM) images of ASG (Fig. 4(a)) and CAMSG (Fig. 4(b)). The elemental analysis of ASG and CAMSG was performed by Elementar Vario EL III, and wt.% of C in ASG and CAMSG was found to be 0.51 and 8.62%, respectively.

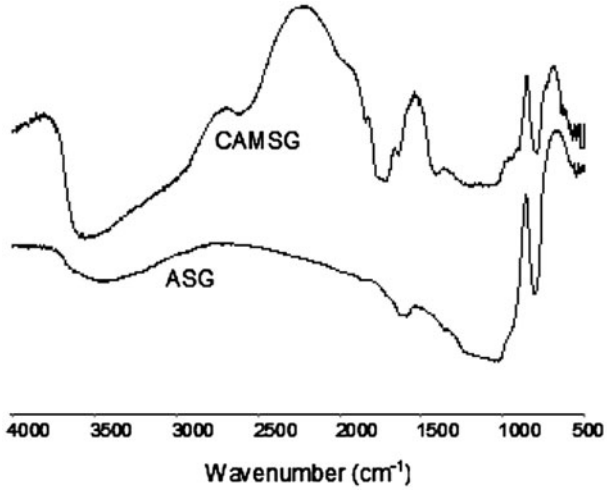

Fig. 3. FT-IR spectra of ASG and CAMSG.

3.2. Influence of initial pH

The influence of pH on the adsorption of MB dye solution was studied over a range of pH 3–11. As shown in Fig. 5, the adsorption of MB increased from 25 to 77% on ASG and from 30 to 96.4% on CAMSG, while the pH increased from 3 to 7. At lower pH values, the hydrogen ion competes with MB dye and most of the hydroxyl groups of ASG and carboxyl of CAMSG exist in the form of –OH and –COOH, respectively, which reduces the adsorbed amounts for MB dye. At higher pH values, more $–O^-$ and $–COO^-$ ions occur, which may enhance electrostatic attraction, hence the adsorption capacity of the adsorbent for MB dyes increases. The MB adsorption on CAMSG was not much significantly increased after pH 7. So pH 7 was used for further experiments. Higher % removal shown by CAMSG was due to the presence of more anionic ($–COO^-$) (acidic) (Eq. (3)) adsorption site than ASG (Eq. (4)).

$$\text{Si–O–H} \rightarrow \text{Si–O}^- + \text{H}^+$$

$$\text{Si–O}^- + \text{MB}^+ \rightarrow \text{Si–O–MB} \quad (3)$$

$$\text{Si–O–COCH}(\text{CH}_2\text{COOH})_2 \rightarrow \text{Si–O–COCH(OH)} \times (\text{CH}_2\text{COO})_2^{2-} + 2\text{H}^+$$

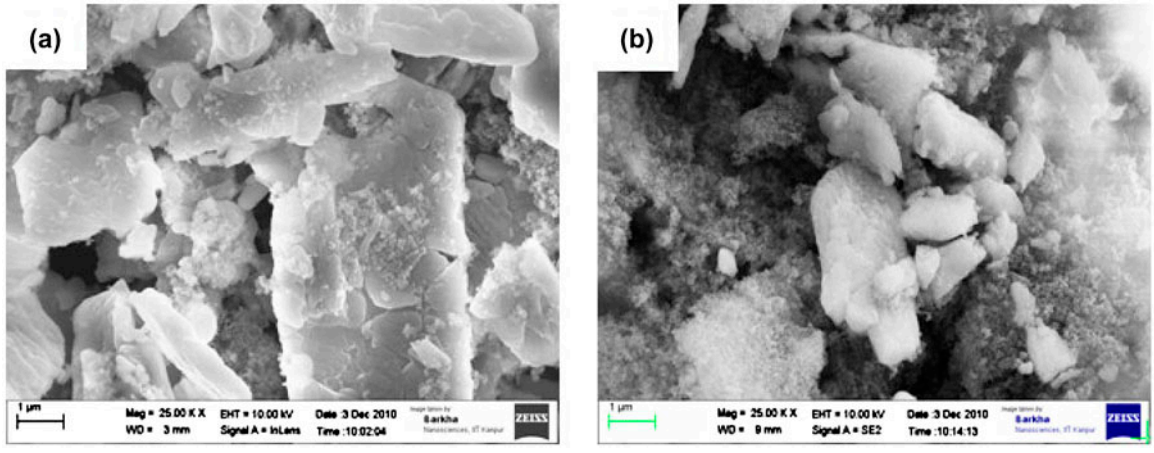

Fig. 4. SEM images of ASG (a) and CAMSG (b).

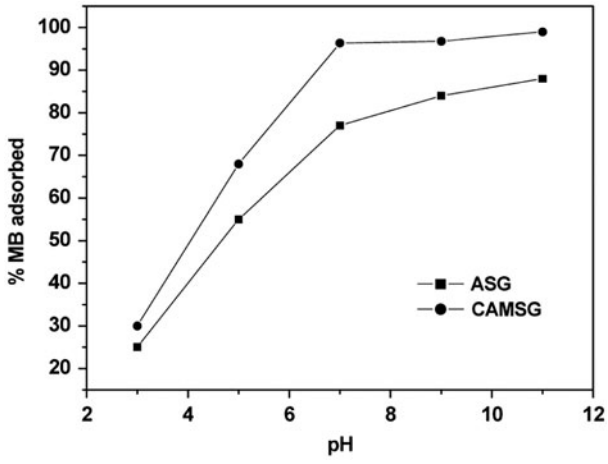

Fig. 5. Influence of pH on adsorption of MB on ASG and CAMSG (adsorbent dose: 2 g/L; initial MB concentration: 100 mg/L; contact time: 100 min; temperature: 303 K).

$$\text{Si–O–COCH(OH)}(\text{CH}_2\text{COO})_2^{2-} + 2\text{MB}^+ \rightarrow \text{Si–O–COCH(OH)}(\text{CH}_2\text{COOMB})_2 \quad (4)$$

3.3. Effect of adsorbent dose

The effect of adsorbent dose on adsorption was studied using different amounts of adsorbent dosage in the range of 0.5–4 g/L. As shown in Fig. 6, by increasing adsorbent dose frequently from 0.5 to 4 g/L, the adsorption of MB on ASG increased from 40 to 85% and in case CAMSG, it increased from 55 to 97% on increasing the dose from 0.5 to 2 g/L. The increase in % adsorption with increase of adsorbent dose was due to the greater availability of the adsorption binding sites. Further increase of adsorbent dose of CAMSG did not cause any significant change because equilibrium was achieved between solution and the solid phase.

3.4. Effect of initial dye concentration

To observe the effect of initial dye concentration on adsorption, experiments were conducted over the wide range of initial dye concentrations (20–150 mg/L). Fig. 7 shows that the adsorption of MB decreases from 87.5 to 58.6% and from 98.6 to 96% for ASG and CAMSG, respectively, on increasing the initial dye concentration from 20 to 150 mg/L. The decrease in % MB adsorption with increase in MB concentration is very little in case of CAMSG, which is because of the availability of a large number of adsorption sites. The decrease in % MB adsorption is more in case of ASG due to the availability of lesser number of adsorption sites.

3.5. Adsorption isotherms

The analysis of the adsorption process requires relevant adsorption equilibria for understanding the adsorption process better. Adsorption equilibrium describes the nature of adsorbate–adsorbent interaction. In the present study, the equilibrium data were analyzed using the Langmuir, Freundlich, and Temkin isotherm models.

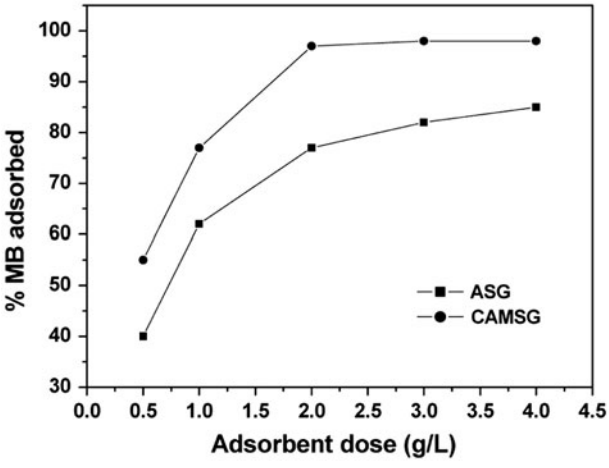

Fig. 6. Influence of adsorbent dose on adsorption of MB on ASG and CAMSG (pH: 7; initial MB concentration: 100 mg/L; contact time: 100 min; temperature: 303 K).

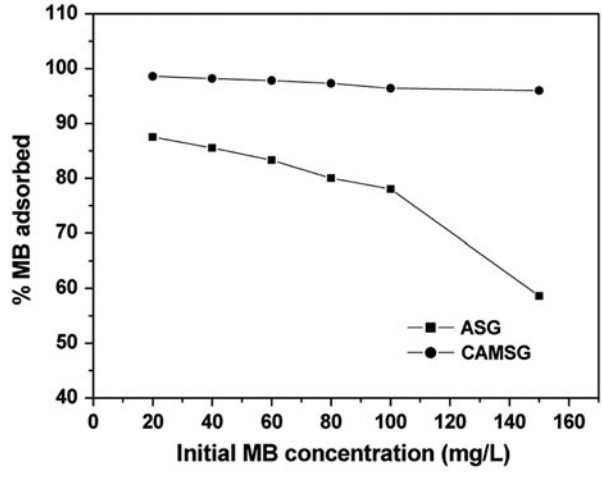

Fig. 7. Influence of initial MB concentration on adsorption of MB on ASG and CAMSG (adsorbent dose: 2 g/L; pH: 7; contact time: 100 min; temperature: 303 K).

3.5.1. Langmuir isotherm model

The saturated monolayer isotherm can be represented by Eq. (5):

$$Q_e = Q_m b C_e/(1 + bC_e) \quad (5)$$

The linearized form of Eq. (5) can be written as [28]:

$$C_e/q_e = 1/bQ_m + C_e/Q_m \quad (6)$$

where q_e is the adsorption density (mg/g) at equilibrium of MB dye, C_e is the equilibrium concentration (mg/L) of the dye in solution, Q_m is the monolayer adsorption capacity (mg/g), and b is the Langmuir constant related to the free energy of adsorption (L/mg). The values of Q_m and b were calculated from the slopes ($1/Q_m$) and the intercepts ($1/bQ_m$) of the linear plots of C_e/q_e vs. C_e (Fig. 8) and are given in Table 1. Linear plots of C_e/q_e vs. C_e show that the adsorption isotherm of MB on ASG and CAMSG follows the Langmuir isotherm model. Table 1 shows higher Q_m value for adsorbent CAMSG which indicates a higher monolayer adsorption capacity for MB than ASG.

3.5.2. Freundlich isotherm model

Freundlich isotherm can be expressed as follows [29]:

$$Q_e = K_f C_e^{1/n} \quad (7)$$

The linearized form of Eq. (7) can be written as follows:

Table 1
Isotherm parameters for MB dye adsorption on ASG and CAMSG

Isotherm parameters	ASG	CAMSG
Langmuir parameters		
Q_{max} (mg/g)	71.42	125.0
b (L/mg)	0.055	0.242
R^2	0.994	0.994
Freundich parameters		
K_f (mg/g (mg/L)$^{-1/n}$)	4.933	24.14
N	1.459	1.644
R^2	0.986	0.987
Temkin parameters		
B	15.28	13.72
b (J/mol)	159.4	183.6
A (L/g)	5.87	0.676
R^2	0.980	0.981

$$\ln q_e = \ln K_f + (1/n) \ln C_e \quad (8)$$

where K_f and n are Freundlich constants related to adsorption capacity [mg g^{-1} (mg L^{-1})$^{-1/n}$] and adsorption intensity of adsorbents. The values of K_f and n were calculated from the intercepts (ln K_f) and the slopes ($1/n$) of the plots ln q_e vs. ln C_e (Fig. 9) and results are presented in Table 1. Linear plots of ln q_e vs. ln C_e show that the adsorption isotherm of MB on ASG and CAMSG also fitted well in the Freundlich isotherm model. Table 1 shows that higher K_f value for CAMSG that indicates a higher adsorption capacity for CAMSG and a value of $n > 1$ indicates favorable adsorption conditions [30,31].

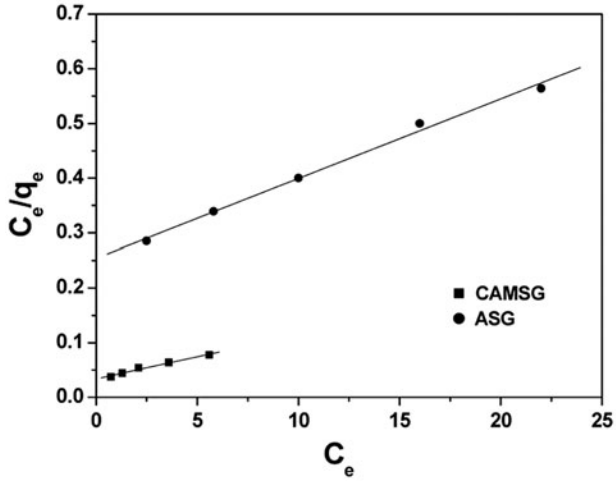

Fig. 8. The Langmuir plots for the adsorption of MB on ASG and CAMSG.

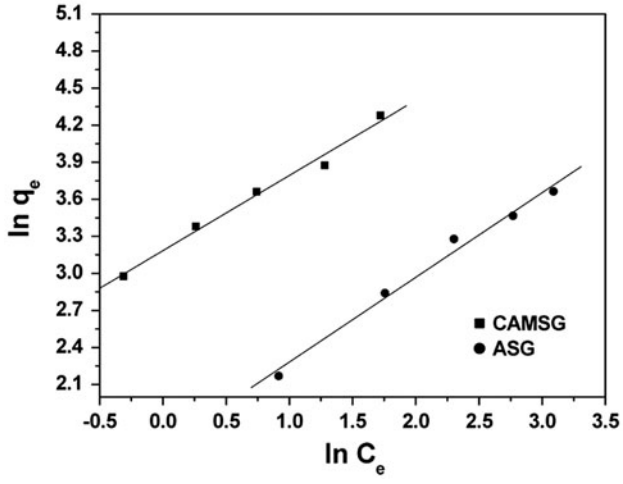

Fig. 9. The Freundlich plots for the adsorption of MB on ASG and CAMSG.

3.5.3. Temkin isotherm model

The derivation of the Temkin isotherm assumes that the fall in the heat of adsorption is linear rather than logarithmic, as implied in the Freundlich equation. The Temkin isotherm can be expressed by Eq. (9) [32]:

$$Q_e = B \ln A + B \ln C_e \quad (9)$$

where $B = RT/b$, b is the Temkin constant (J/mol) related to adsorption heat, T is the absolute temperature (K), R is the gas constant (8.314 J/(mol K), and A is the Temkin isotherm constant (L/g). B and A can be calculated from the slopes (B) and intercepts (B ln A) of the plot of q_e vs. ln C_e (Fig. 10). The Temkin constants B, b, and A together with the R^2 values are shown in Table 1. The heat of adsorption of all the molecules in the layer would decrease linearly with coverage due to adsorbate/adsorbate interactions.

3.6. Adsorption kinetics

Adsorption kinetics were studied for adsorption of MB of initial concentration range, 20, 40, 60, 80, and 100 mg/L on ASG and 40, 60, 80, 100, and 150 mg/L on CAMSG. Figs. 11 and 12 show that the rate of adsorption decreases with increase in time and after 100 min, equilibrium was achieved.

Several kinetic models have been proposed to clarify the mechanism of a solute adsorption from aqueous solution onto an adsorbent. The rate constant of adsorption was determined from the pseudo-first-order rate expression (Eq. (10)) [33] given by Lagergren:

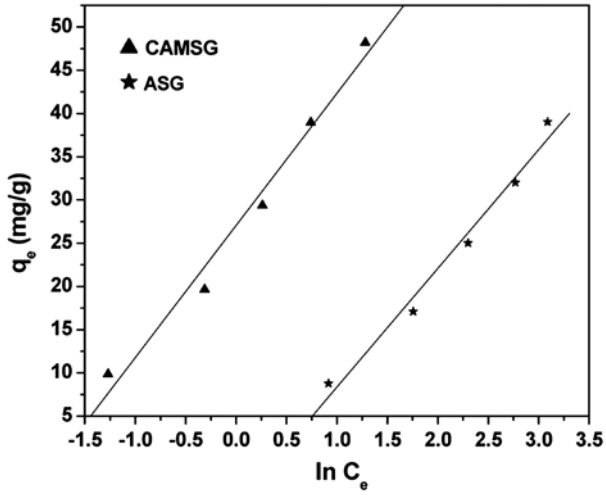

Fig. 10. The Temkin plots for the adsorption of MB on ASG and CAMSG.

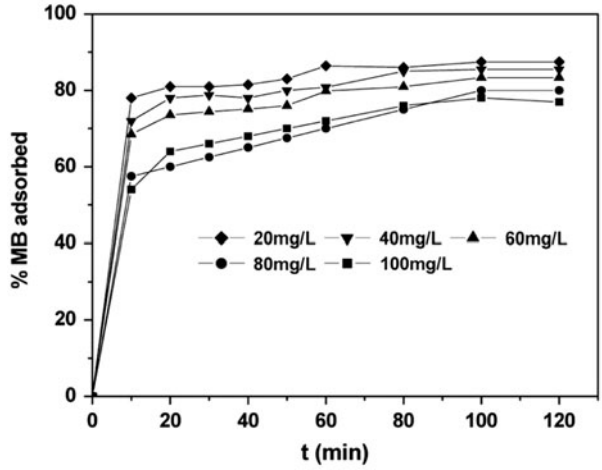

Fig. 11. Sorption kinetics of MB on ASG (adsorbent dose: 2 g/L; pH: 7; temperature: 303 K).

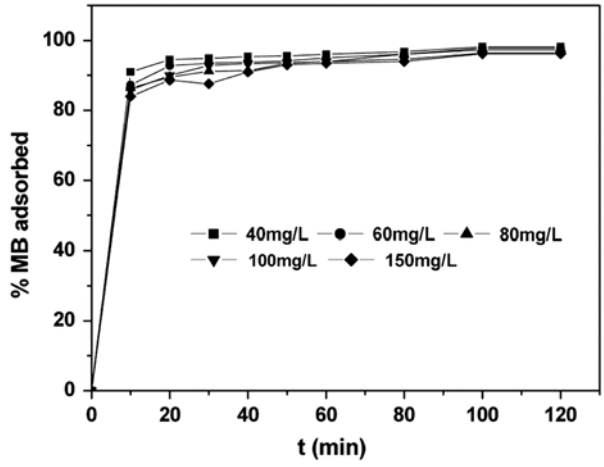

Fig. 12. Sorption kinetics of MB on CAMSG (adsorbent dose: 2 g/L; pH: 7; temperature: 303 K).

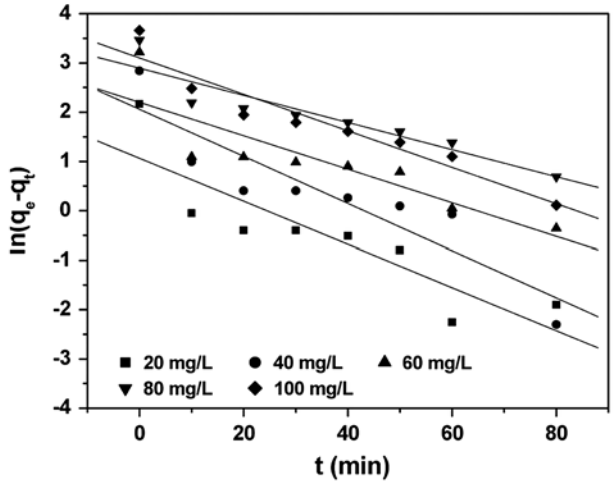

Fig. 13. Pseudo-first-order kinetics plots for adsorption of MB on ASG (adsorbent dose: 2 g/L; pH: 7; temperature: 303 K).

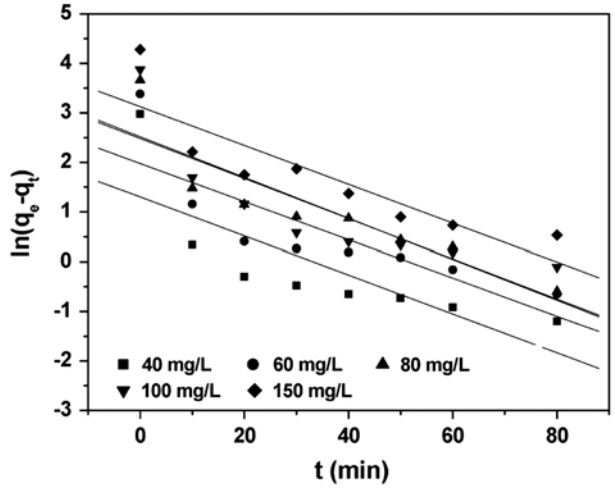

Fig. 14. Pseudo-first-order kinetics plots for adsorption of MB on CAMSG (adsorbent dose: 2 g/L; pH: 7; temperature: 303 K).

$$\ln(q_e - q_t) = \ln q_e - k_{ad}t \quad (10)$$

where q_e and q_t are the amount of MB adsorbed at equilibrium and at time t (mg/g), respectively, and k_{ad} (min^{-1}) is rate constant of adsorption. The values of the k_{ad} and q_e^{cal} were calculated from the slopes ($-k_{ad}$) and the intercepts (ln q_e) of the plots of ln ($q_e - q_t$) vs. t (Figs. 13 and 14), respectively, and are reported in Table 2. As shown in Table 2, the values of regression correlation coefficients (R^2) are not close to unity and a large difference in the values of q_e^{cal} and q_e^{exp} for both the adsorbents concluded that the pseudo-first-order model is not suitable to describe the kinetic profile of the adsorption.

The pseudo-second-order adsorption kinetics [33] may be written as Eq. (11):

$$t/q_t = 1/k_2 q_e^2 + t/q_e \quad (11)$$

where k_2 is the rate constant of adsorption(g/mg min), q_e and q_t are the amount of MB adsorbed at equilibrium and at time t (mg/g), respectively. The values of k_2 and q_e^{cal} were calculated from the intercepts ($1/k_2 q_e^2$) and the slopes ($1/q_e$) of the plots of t/q_t vs. t. (Figs. 15 and 16), respectively, and are reported in Table 2. The results show that the values of regression correlation coefficients (R^2) are close to unity and the values of q_e^{cal} and q_e^{exp} are almost equal which confirm that the adsorption of MB on to ASG and CAMSG follows a pseudo-second-order kinetic model.

The mechanism of adsorption can be explained by an intraparticle diffusion model [34]. The equation for intraparticle diffusion can be expressed by Eq. (12):

$$Q_t = k_i t^{0.5} + C \quad (12)$$

where k_i is the intraparticle diffusion constant (mg/g $min^{0.5}$) and the intercept (C) reflects the boundary-layer effect. The values of k_i were calculated from the slopes (k_i) of the plots of q_t vs. $t^{0.5}$ (Figs. 17 and 18), and are presented in Table 2.

Table 2 shows that the rate constant for intraparticle diffusion (k_i) increased with the increasing initial MB dye concentration. The driving force of diffusion

Table 2
Kinetic parameters for MB dye adsorption on ASG and CAMSG

Initial dye concentration	q_e^{exp}	Pseudo-first-order			Pseudo-second-order			Intraparticle diffusion		
		q_e^{cal}	k_{ad}	R^2	q_e^{cal}	k_2	R^2	k_i	C	R^2
ASG										
20 mg/L	8.75	2.89	0.043	0.762	8.77	0.067	0.998	0.138	7.382	0.916
40 mg/L	17.10	7.80	0.047	0.818	17.54	0.029	0.999	0.409	13.25	0.860
60 mg/L	25.00	9.00	0.034	0.744	25.64	0.014	0.997	0.616	18.84	0.956
80 mg/L	32.00	18.0	0.027	0.859	32.25	0.0055	0.986	1.321	18.09	0.975
100 mg/L	39.00	22.0	0.037	0.912	40.00	0.0054	0.994	1.669	23.26	0.945
CAMSG										
40 mg/L	19.63	3.60	0.039	0.618	20.00	0.021	0.994	0.171	17.91	0.879
60 mg/L	29.35	7.20	0.038	0.684	29.41	0.015	0.993	0.379	25.62	0.853
80 mg/L	38.95	12.40	0.041	0.791	40.00	0.015	0.999	0.619	32.85	0.983
100 mg/L	48.20	11.97	0.040	0.701	50.00	0.010	0.997	0.678	41.76	0.842
150 mg/L	72.20	22.70	0.039	0.763	71.42	0.010	0.994	1.277	59.75	0.928

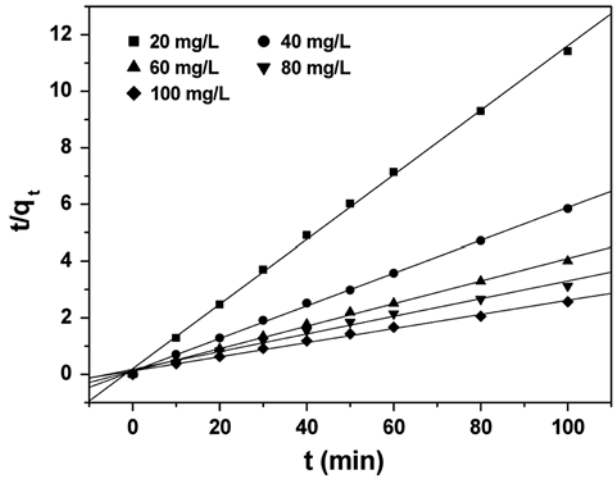

Fig. 15. Pseudo-second-order kinetics plots for adsorption of MB on ASG (adsorbent dose: 2 g/L; pH: 7; temperature: 303 K).

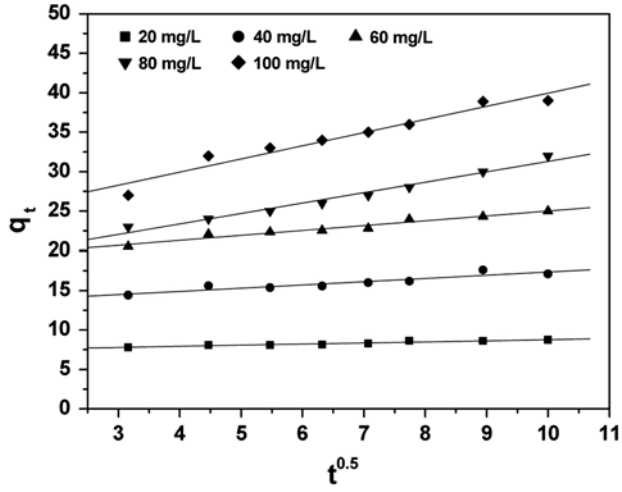

Fig. 17. Intraparticle diffusion plots for the adsorption of MB from aqueous solution on ASG (adsorbent dose: 2 g/L; pH: 7; temperature: 303 K).

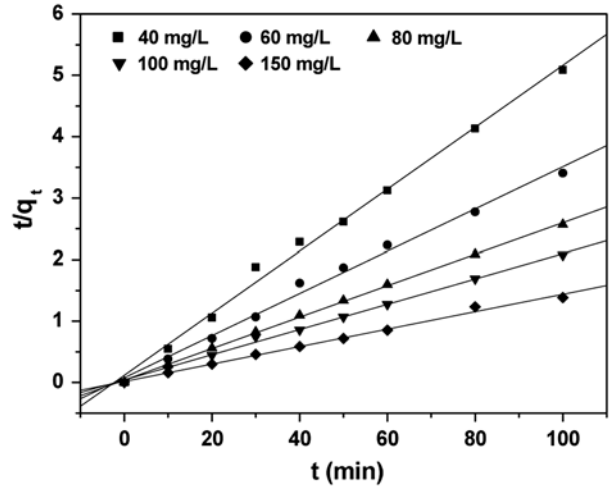

Fig. 16. Pseudo-second-order kinetics plots for adsorption of MB on CAMSG (adsorbent dose: 2 g/L; pH: 7; temperature: 303 K).

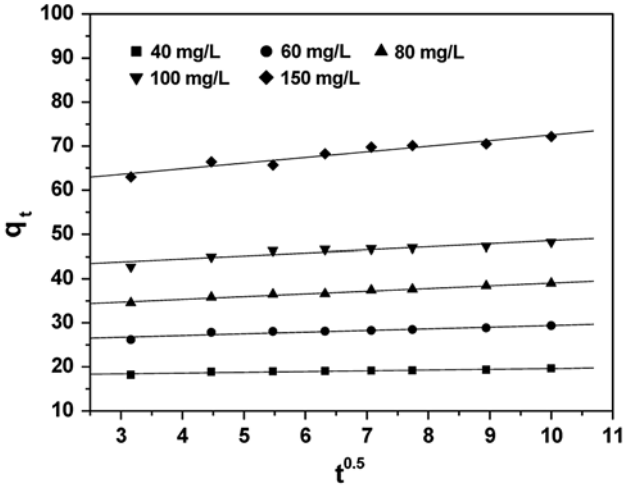

Fig. 18. Intraparticle diffusion plots for the adsorption of MB from aqueous solution on CAMSG (adsorbent dose: 2 g/L; pH: 7; temperature: 303 K).

is very important for adsorption processes. The increase of the initial dye concentration results in an increase in the driving force, which will increase the diffusion rate of MB [35]. Figs. 17 and 18 revealed that the lines of plots are not passing through the origin. Table 2 shows that the values of C increase with an increase in the initial concentration of MB. Larger the value of C, greater is the contribution of the surface adsorption in the rate-limiting step, confirms the presence of both surface adsorption and intraparticle diffusion [36].

3.7. Thermodynamic studies

To observe the effect of temperature on the adsorption of MB on ASG and CAMSG, experiments were conducted at three different temperatures 303, 313, and 323 K. It was observed that the adsorption decreases with increasing temperature for both the adsorbents which indicates that a low temperature favors MB adsorption onto ASG and CAMSG adsorbent. This may be due to a tendency for the MB molecules to escape from the solid phase to the bulk phase with an increase in temperature of the solution.

Table 3
Thermodynamic parameters for MB dye adsorption on ASG and CAMSG

Initial dye concentration	ΔH° (kJ/mol)	ΔS° (J/mol/K)	ΔG° (kJ/mol)		
			303 K	313 K	323 K
ASG					
20 mg/L	−41.769	−121.55	−4.939	−3.723	−2.508
40 mg/L	−39.616	−115.64	−4.577	−3.420	−2.248
60 mg/L	−34.228	−99.35	−4.124	−3.131	−2.137
80 mg/L	−25.873	−73.72	−3.535	−2.798	−2.061
100 mg/L	−21.782	−61.62	−3.111	−2.494	−1.878
CAMSG					
40 mg/L	−43.440	−109.82	−10.164	−9.066	−7.968
60 mg/L	−44.953	−116.31	−9.711	−8.547	−7.384
80 mg/L	−41.894	−107.66	−9.273	−8.196	−7.119
100 mg/L	−36.714	−94.11	−8.198	−7.257	−6.316
150 mg/L	−39.408	−103.50	−8.047	−7.012	−5.977

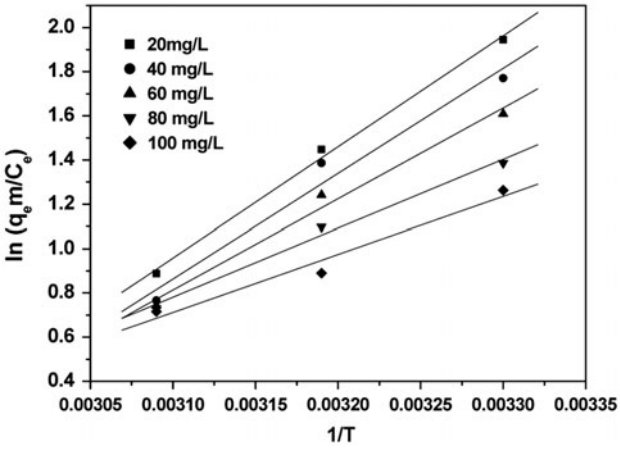

Fig. 19. The plots of ln ($q_e m/C_e$) vs. $1/T$ for adsorption of MB on ASG (adsorbent dose: 2 g/L; pH: 7; time 100 min).

A similar observation was also reported in the study on the sorption of cadmium onto oxidized granular-activated carbon [37].

Thermodynamic parameters such as enthalpy (ΔH°), entropy (ΔS°) and Gibb's free energy (ΔG°) were determined by Eqs. (13) and (14) [38].

$$\ln(q_e m/C_e) = \Delta S^\circ/R - \Delta H^\circ/RT \quad (13)$$

$$\Delta G^\circ = \Delta H^\circ - T\Delta S^\circ \quad (14)$$

where m is the adsorbent dose (g/L), C_e is the equilibrium concentration (mg/L) of the MB in solution, q_e is the amount of MB adsorbed at equilibrium (mg/g),

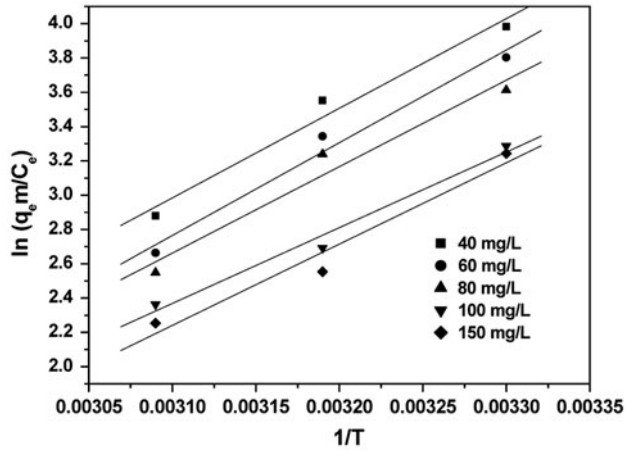

Fig. 20. The plots of ln ($q_e m/C_e$) vs. $1/T$ for adsorption of MB on CAMSG (adsorbent dose: 2 g/L; pH: 7; time: 100 min).

and $q_e m$ is the solid phase concentration (mg/L) at equilibrium. R is the gas constant (8.314 J/mol/K) and T is the temperature (K). ΔH°, ΔS°, and ΔG° are changes in enthalpy (J/mol), entropy (J/mol/K), and Gibb's free energy (J/mol), respectively.

The values of ΔH° and ΔS° were determined from the slopes ($-\Delta H^\circ/R$) and the intercept ($\Delta S^\circ/R$) of the plots of ln ($q_e m/C_e$) vs. $1/T$ (Figs. 19 and 20). The ΔG° values were calculated using Eq. (14). The values of thermodynamic parameters are presented in Table 3. Negative values of ΔG° indicate that the adsorption process is feasible and spontaneous in nature. Negative values of ΔH° suggest the exothermic nature of adsorption and the negative values of ΔS° describe the randomness at the adsorbent–solution interface decreased during the adsorption. The ΔH° values obtained for the adsorption of MB on ASG and CAMSG are in the range of –21.78 to –41.76 kJ/mol and –39.40 to –44.95 kJ/mol, respectively, which indicate the presence of both physical and chemical adsorption mechanism. However, the chemisorption was more predominant on CAMSG than ASG.

4. Conclusions

The present study shows that the CAMSG is a potential adsorbent for the effective removal of MB dye from aqueous solution. The pH 7 and temperature 303 K was found to be optimum for adsorption study. The removal% of MB dye increased from 75 to 95% after chemical modification of SG with CA. Equilibrium study shows that the adsorption of MB on ASG and CAMSG are fitted well in Langmuir and Freundlich isotherm models. Kinetics study shows that the rate of adsorption decrease with increase in

time and equilibrium was achieved within 100 min of contact time. It was found that the pseudo-second-order kinetics fitted better than the pseudo-first-order kinetics. Two mechanisms intraparticle diffusion and surface sorption were found to be involved in the rate-determining step of the sorption of the MB dye from solution. The thermodynamic study shows that the adsorption process was exothermic and spontaneous in nature for both the adsorbents.

Acknowledgments

The authors are thankful to Dr. Dinesh Deva of Nanoscience, IIT Kanpur, India for recording SEM and Council of Scientific and Industrial Research (CSIR), New Delhi, India, for the financial support.

References

[1] M.X. Zhu, L. Lee, H.H. Wang, Z. Wang, Removal of an anionic dye by adsorption/precipitation processes using alkaline white mud, J. Hazard. Mater. 149 (2007) 735–741.
[2] S.S. Moghaddam, M.R.A. Moghaddam, M. Arami, Coagulation/flocculation process for dye removal using sludge from water treatment plant: Optimization through response surface methodology, J. Hazard. Mater. 175 (2010) 651–657.
[3] D.J. Chang, I.P. Chen, M.T. Chen, S.S. Lin, Wet air oxidation of a reactive dye solution using CoAlPO4-5 and CeO_2 catalysts, Chemosphere 52 (2003) 943–949.
[4] S.M. Ghoreishi, R. Haghighi, Chemical catalytic reaction and biological oxidation for treatment of non-biodegradable textile effluent, Chem. Eng. J. 95 (2003) 163–169.
[5] S. Raghu, C.W. Lee, S. Chellammal, S. Palanichamy, C.A. Basha, Evaluation of electrochemical oxidation techniques for degradation of dye effluents—A comparative approach, J. Hazard. Mater. 171 (2009) 748–754.
[6] K.M.M. Nowak, Application of ceramic membranes for the separation of dye particles, Desalination 254 (2010) 185–191.
[7] L. Zheng, Y. Su, L. Wang, Z. Jiang, Adsorption and recovery of methylene blue from aqueous solution through ultrafiltration technique, Sep. Purif. Technol. 68 (2009) 244–249.
[8] I.A. Salem, Md.S. El-Maazawi, Kinetics and mechanism of color removal of methylene blue with hydrogen peroxide catalyzed by some supported alumina surfaces, Chemosphere 41 (2000) 1173–1180.
[9] C.H. Weng, Y.F. Pan, Adsorption of a cationic dye (methylene blue) onto spent activated clay, J. Hazard. Mater. 144 (2007) 355–362.
[10] A.C. Suwandi, N. Indraswati, S. Ismadji, Adsorption of N-methylated diaminotriphenilmethane dye (malachite green) on natural rarasaponin modified kaolin, Desalin. Water Treat. 41 (2012) 342–355.
[11] J.X. Lin, L. Wang, Treatment of textile wastewater using organically modified bentonite, Desalin. Water Treat. 25 (2011) 25–30.
[12] C. Yan, C. Wang, J. Yao, L. Zhang, X. Liu, Adsorption of methylene blue on mesoporous carbons prepared using acid- and alkaline-treated zeolite X as the template, Colloids Surf. A: Physicochem. Eng. Asp. 333 (2009) 115–119.
[13] A.N. Fernandesa, C.A.P. Almeida, C.T.B. Menezes, N.A. Debacher, M.M.D. Sierra, Removal of methylene blue from aqueous solution by peat, J. Hazard. Mater. 144 (2007) 412–419.
[14] S. Altenora, B. Carenea, E. Emmanuel, J. Lambert, J.J. Ehrhardt, S. Gasparda, Adsorption studies of methylene blue and phenol onto vetiver roots activated carbon prepared by chemical activation, J. Hazard Mater. 165 (2009) 1029–1039.
[15] M. Zhao, Z. Tang, P. Liu, Removal of methylene blue from aqueous solution with silica nano-sheets derived from vermiculite, J. Hazard. Mater. 158 (2008) 43–51.
[16] D. Zhao, L. Zhao, C.S. Zhu, X. Shen, X. Zhang, B. Sha, Comparative study of polymer containing β-cyclodextrin and –COOH for adsorption toward aniline, 1-naphthylamine and methylene blue, J. Hazard. Mater. 171 (2009) 241–246.
[17] M.C. Ncibi, A.M.B. Hamissa, A. Fathallah, M.H. Kortas, T. Baklouti, B. Mahjoub, M. Seffen, Biosorptive uptake of methylene blue using Mediterranean green alga *Enteromorpha* spp., J. Hazard. Mater. 170 (2009) 1050–1055.
[18] R. Han, Y. Wang, X. Zhao, Y. Wang, F. Xie, J. Cheng, M. Tang, Adsorption of methylene blue by phoenix tree leaf powder in a fixed-bed column: Experiments and prediction of breakthrough curves, Desalination 245 (2009) 284–297.
[19] V. Ponnusami, S. Vikram, S.N. Srivastava, Guava (Psidium guajava) leaf powder: Novel adsorbent for removal of methylene blue from aqueous solutions, J. Hazard. Mater. 152 (2008) 276–286.
[20] R. Srivastava, D.C. Rupainwar, Eucalyptus bark powder as an effective adsorbent: Evaluation of adsorptive characteristics for various dyes, Desalin. Water Treat. 11 (2009) 302–313.
[21] A.E. Ofomaja, Equilibrium sorption of mehtylene blue using mansonia wood sawdust as biosorbent, Desalin. Water Treat. 3 (2009) 1–10.
[22] B.H. Hameed, A.A. Ahmad, Batch adsorption of methylene blue from aqueous solution by garlic peel, an agricultural waste biomass, J. Hazard. Mater. 164 (2009) 870–875.
[23] R. Han, L. Zhang, C. Song, M. Zhang, H. Zhu, L. Zhang, Characterization of modified wheat straw, kinetic and equilibrium study about copper ion and methylene blue adsorption in batch mode, Carbohydr. Polym. 79 (2010) 1140–1149.
[24] L. Wang, J. Zhang, A. Wang, Removal of methylene blue from aqueous solution using chitosan-g-poly (acrylic acid)/montmorillonite super adsorbent nanocomposite, Colloids Surf. A: Physicochem. Eng. Asp. 322 (2008) 47–53.
[25] Y. Liu, Y. Zheng, A. Wang, Enhanced adsorption of methylene blue from aqueous solution by chitosan-g-poly (acrylic acid)/vermiculite hydrogel composites, J. Environ. Sci. 22 (2010) 486–493.
[26] L. Xionga, Y. Yang, J. Maia, W. Suna, C. Zhang, D. Weic, Q. Chen, J. Nia, Adsorption behavior of methylene blue onto titanate nanotubes, Chem. Eng. J. 156 (2010) 313–320.
[27] T. Vaughan, C.W. Sew, W.E. Marshall, Removal of selected metal ions from aqueous solution using modified corncobs, Bioresour. Technol. 78 (2001) 133–139.
[28] M. Ghoul, M. Bacquet, M. Morcellet, Uptake of heavy metals from synthetic aqueous solutions using modified PEI—silica gels, Water Res. 37 (2003) 729–734.
[29] A. Aklil, M. Mouflih, S. Sebti, Removal of heavy metal ions from water by using calcined phosphate as a new adsorbent, J. Hazard. Mater. A 112 (2004) 183–190.
[30] B.H. Hameed, D.K. Mahmoud, A.L. Ahmad, Equilibrium modeling and kinetic studies on the adsorption of basic dye by a low-cost adsorbent: Coconut (*Cocos nucifera*) bunch waste, J. Hazard. Mater. 158 (2008) 65–72.
[31] B.H. Hameed, Grass waste: A novel sorbent for the removal of basic dye from aqueous solution, J. Hazard. Mater. 166 (2009) 233–238.
[32] V.S. Mane, I.D. Mall, V.C. Srivastava, Kinetic and equilibrium isotherm studies for the adsorptive removal of brilliant green dye from aqueous solution by rice husk ash, J. Environ. Manage. 84 (2007) 390–400.
[33] M. Dogan, M. Alkan, A. Türkyilmaz, Y. Özdemir, Kinetics and mechanism of removal of methylene blue by adsorption onto perlite, J. Hazard. Mater. B 109 (2004) 141–148.
[34] Y. Zhi-yuan, Kinetics and mechanism of the adsorption of methylene blue onto ACFs, J. China Univ. Mining Technol. 18 (2008) 0437–0440.

[35] C.H. Weng, Y.F. Pan, Adsorption characteristics of methylene blue from aqueous solution by sludge ash, Colloids Surf. A: Physicochem. Eng. Asp. 274 (2006) 154–162.
[36] K.V. Kumar, K. Porkodi, Mass transfer, kinetics and equilibrium studies for the biosorption of methylene blue using Paspalum notatum, J. Hazard. Mater. 146 (2007) 214–226.
[37] X. Huang, N. Gao, Q. Zhang, Thermodynamics and kinetics of cadmium adsorption onto oxidized granular activated carbon, J. Environ. Sci. 19 (2007) 1287–1292.
[38] B.K. Nandi, A. Goswami, M.K. Purkait, Adsorption characteristics of brilliant green dye on kaolin, J. Hazard. Mater. 161 (2009) 387–395.